

# PyKirigami: An interactive Python simulator for kirigami structures

Qinghai Jiang<sup>1</sup>, Gary P. T. Choi<sup>1,\*</sup>

<sup>1</sup>Department of Mathematics, The Chinese University of Hong Kong

\*To whom correspondence should be addressed; E-mail: ptchoi@cuhk.edu.hk

## Abstract

In recent years, the concept of kirigami has been used in creating deployable structures for various scientific and technological applications. While high-fidelity Finite Element Analysis (FEA) is the standard for analyzing stress distributions and material deformation, it is computationally intensive and often ill-suited for the rapid exploration of vast kinematic configuration spaces. In this work, we develop PyKirigami, a lightweight, open-source Python framework for the efficient deployment simulation of kirigami structures. Unlike continuum mechanics solvers, PyKirigami models tessellations as articulated rigid-body networks, allowing for the real-time simulation of global deployment trajectories and volumetric transformations. The tool incorporates collision detection and interactive actuation, enabling users to validate folding paths and identify geometric locking states in both 2D and 3D topologies. This framework serves as a fast kinematic prototyping tool for kirigami structures, allowing researchers to verify deployment mechanics and self-contacts prior to performing detailed mechanical analysis or physical fabrication.

## 1 Introduction

Kirigami, the traditional paper-cutting art, has recently become a subject of great interest in science and engineering [1–6]. In particular, a wide range of deployable structures with different shape-morphing effects have been developed by introducing cuts on a sheet of materials and connecting different components using suitable joints. Because of their great flexibility and shape-shifting property, kirigami-based structures have been widely applied in soft electronics [7], energy storage [8], and robotics [9].

Most prior works on kirigami design have focused on planar deployable structures and their in-plane deformations based on simple cutting patterns, such as rotating triangles [10], quadrilaterals [11, 12], and other periodic tilings [13–15] and aperiodic tilings [16]. In recent years, some works have also explored the design of more general kirigami patterns for

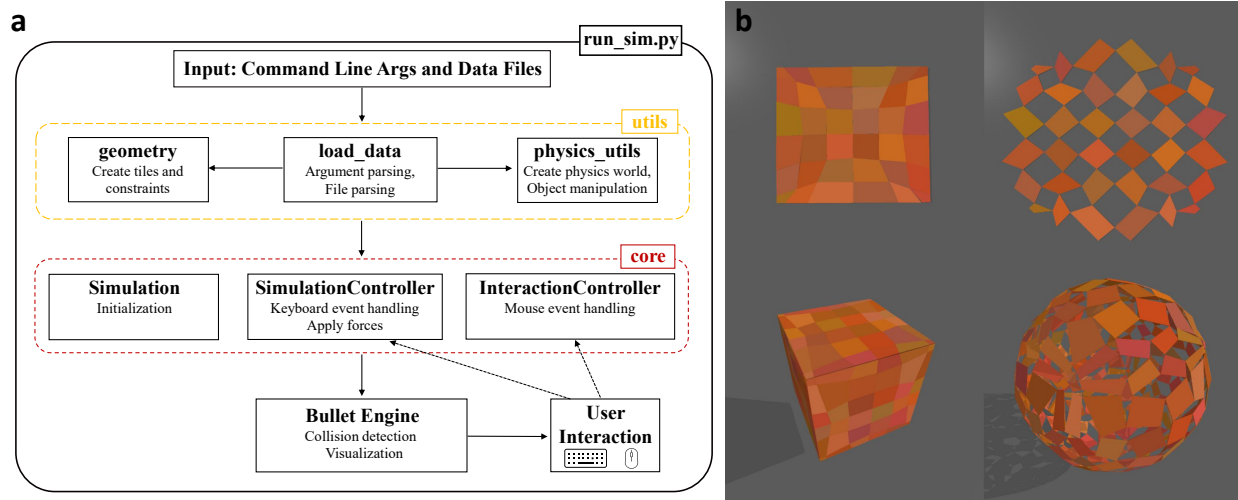


Figure 1: **An overview of PyKirigami.** **a**, The computational framework of PyKirigami. **b**, Using PyKirigami, one can easily simulate the deployment process of different kirigami structures in 2D (top) and 3D (bottom).

achieving different physical and geometrical effects [17–26]. There is also an increasing interest in designing kirigami for achieving not just two-dimensional (2D) but three-dimensional (3D) shape transformations with different desired 2D-to-3D or 3D-to-3D shape-morphing effects [27–34].

While the design of kirigami structures has been extensively studied, computational methods for the simulation and analysis of their shape-morphing process are much less explored. Most prior kirigami design works directly used finite element analysis (FEA) software such as ABAQUS (e.g., [26, 35, 36]) or COMSOL (e.g., [37–39]) to simulate the deployment process of kirigami structures under certain boundary loading conditions. Some other works considered other mechanical models involving linear springs for simulating 2D-to-2D and 2D-to-3D deployments in MATLAB [18, 20]. More recently, Liu et al. [16] developed a 2D-to-2D kirigami deployment simulator in Python based on the 2D rigid body physics library Pymunk, with a focus on rigidly deployable planar kirigami patterns. However, in many practical applications, it is necessary to simulate more general kirigami deployment processes in both 2D and 3D. Also, one may need to consider not just the kirigami structures but also their interactions with the environment and external objects throughout the deployment. Moreover, it is highly desirable to have a lightweight, efficient, and freely available deployment simulator with interactive control functionalities that allow for real-time manipulation and analysis of kirigami structures.

In this work, we develop PyKirigami, an open-source Python-based simulator, for simulating the 2D and 3D deployment of general kirigami structures (Fig. 1). Specifically, our simulator utilizes the PyBullet physics engine [40] and is capable of simulating 2D-to-2D, 2D-to-3D, and 3D-to-3D kirigami deployments. It also supports the configurations of environmental effects and stabilization mechanisms for modelling different scenarios. It further allows dynamic

control of the boundary conditions throughout the deployment process, thereby providing great flexibility in achieving different desired deployment effects. Using PyKirigami, one can easily simulate the deployment and analyze the properties of a wide range of kirigami structures.

## 2 Methods

### 2.1 Overview

The goal of our PyKirigami simulator is to simulate the deployment process of kirigami structures, typically from a compact initial state to a deployed configuration in either 2D or 3D. More specifically, the functionalities of PyKirigami (Fig. 1a) can be categorized as follows:

- **Core Simulation Logic:** This component is responsible for the main simulation loop, handling physics calculations, and managing the state of the simulated objects. It includes classes for managing the simulation state, handling user interactions (like pausing and resetting), and applying forces to the objects.
- **Utility Functions:** This group contains modules for parsing command-line arguments, loading input data (such as vertex coordinates and constraints), and performing geometric operations like creating 3D models from 2D definitions.
- **Main Executable:** The main executable script initializes the simulation environment, orchestrates the simulation loop, and integrates the various modules.

The core concepts in PyKirigami are presented in further detail in the following sections. See also Appendix A–B for more detailed explanations.

### 2.2 Geometric Representation: From 2D Polygons to 3D Tiles

In our work, we consider polygonal tiles formed by straight cuts, noting that curved cuts can be discretized and approximated using multiple straight cuts in practical applications. Also, in prior works on kirigami design and simulation [16, 18], the kirigami tiles were commonly considered as two-dimensional objects with zero thickness for simplicity. By contrast, here we consider the kirigami tiles as 3D rigid bodies (“bricks”) in both the in-plane and 3D deployment simulations, thereby enabling a more realistic simulation process.

More mathematically, let  $\{\mathcal{T}_i\}_{i=1}^N$  be the collection of all kirigami tiles in a kirigami structure, where each tile  $\mathcal{T}_i$  is initially defined by a sequence of vertices  $\{v_{i,1}, v_{i,2}, \dots, v_{i,n_i}\}$ , where  $v_{i,j} \in \mathbb{R}^3$  and  $n_i$  is the number of vertices for tile  $\{\mathcal{T}_i\}$  (see also Fig. 2a). To create a more physically realistic model, each planar tile is extruded into a 3D rigid body, or “brick,” with a user-defined thickness,  $t$ . This process is detailed in Algorithm 1 and illustrated in Fig. 2b. See also Appendix B for more details of the geometric representation.

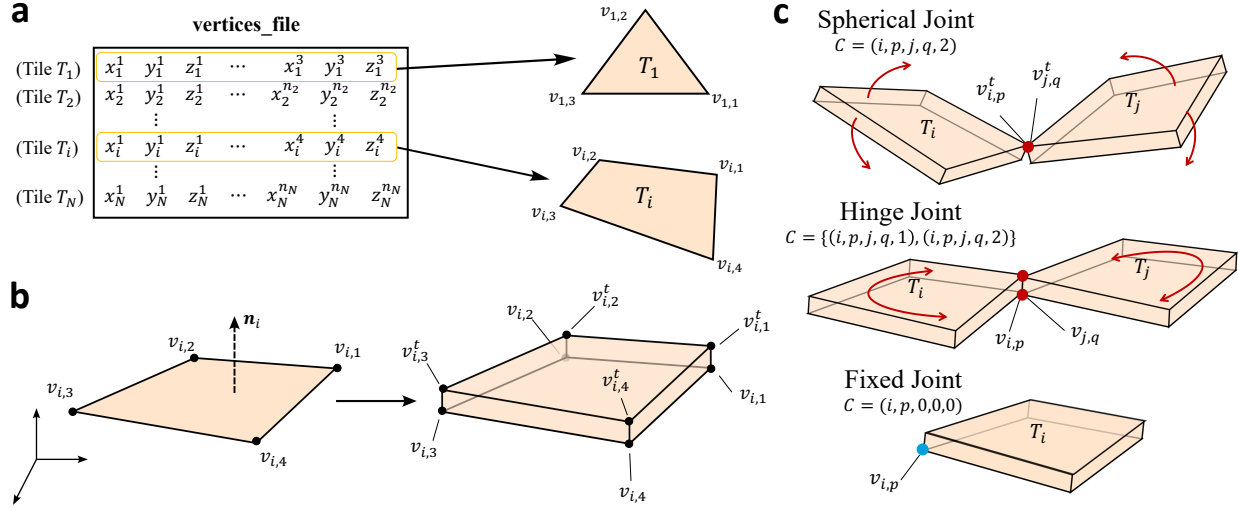


Figure 2: **Tile construction and connections in PyKirigami.** **a**, An illustration of the vertex coordinates encoded in the input file via `--vertices_file`. Here, note that different tiles may contain different number of vertices. **b**, Geometric construction of the 3D kirigami tiles. (Left) The original polygonal tile  $\mathcal{T}_i$ , with the dotted arrow showing its normal vector. (Right) The 3D tile geometry constructed by extruding  $\mathcal{T}_i$  along its normal vector. Here, the thickness of the tile can be prescribed by the user. **c**, Three different types of inter-tile connections in PyKirigami. (Top) Spherical joint applied to tiles  $\mathcal{T}_i$  and  $\mathcal{T}_j$  such that the rotational degree of freedom equals 3. (Middle) Hinge joint such that the rotational degree of freedom equals 1. (Bottom) Fixed joint applied to  $\mathcal{T}_i$  and world frame such that the object is totally fixed. The arrow represents the rotational degree of freedom.

---

### Algorithm 1 3D Tile Generation Pipeline

---

- 1: **Input:** Vertex coordinates file, brick thickness parameter  $t$
  - 2: **Output:** PyBullet body IDs, local vertex coordinates for each tile
  - 3: Load vertex data from input file
  - 4: **for** each tile  $\mathcal{T}_i$  with vertices  $\{v_{i,1}, v_{i,2}, \dots, v_{i,n_i}\}$  **do**
  - 5:   Compute geometric center:  $\mathbf{c}_i = \frac{1}{n_i} \sum_{j=1}^{n_i} v_{i,j}$ .
  - 6:   Calculate normal vector:  $\mathbf{n}_i = \frac{(v_{i,2}-v_{i,1}) \times (v_{i,3}-v_{i,1})}{\|(v_{i,2}-v_{i,1}) \times (v_{i,3}-v_{i,1})\|}$ .
  - 7:   Generate top vertices:  $v_{i,j}^t = v_{i,j} + t \cdot \mathbf{n}_i$  for  $j = 1, \dots, n_i$ .
  - 8:   Store local coordinates:  $v_{i,j} - \mathbf{c}_i$  and  $v_{i,j}^t - \mathbf{c}_i$ .
  - 9:   Create visual mesh and collision shape from  $2n_i$  vertices.
  - 10:   Instantiate rigid body in physics engine, return body ID.
  - 11: **end for**
-

## 2.3 Kinematic Connections: Modeling Joints with Constraints

The connections between tiles in kirigami structures are crucial for their kinematic behavior. Building upon existing work, we adopt and extend the constraint representation framework introduced in [16].

**Extension from 2D to 3D Constraint Representation** In the prior 2D work [16], each constraint is represented as a 4-tuple  $\mathcal{C}_k = (i, p, j, q)$ , which enforces that vertex  $p$  of tile  $i$  coincides with vertex  $q$  of tile  $j$ . This constraint effectively creates a spherical joint in 2D space such that

$$v_{i,p} = v_{j,q}. \quad (1)$$

Extending this to 3D naturally requires an additional  $z$ -coordinate constraint. However, since our tiles are 3D rigid bodies with distinct top and bottom faces, we must specify which face contains the connection point. We therefore extend the constraint representation to a 5-tuple  $\mathcal{C}_k = (i, p, j, q, t)$ , where  $t$  is a face specifier:  $t = 1$  for bottom face connections and  $t = 2$  for top face connections. For backward compatibility, if  $t$  is omitted (4-tuple format), we default to bottom face connection.

**Joint Types and Their Implementation** By strategically combining different joints in PyBullet, we can realize different types of kinematic connections with varying degrees of freedom. Each connection type corresponds to a specific pattern of vertex coincidence constraints (see Fig. 2c):

- **Spherical Joint:** The fundamental connection type, implemented using a single point-to-point constraint that enforces coincidence of one vertex from each tile (Fig. 2c, top). This creates a ball-and-socket joint allowing three rotational degrees of freedom around the pivot point.
- **Hinge Joint:** Another connection type constructed using two spherical joints to constrain rotation to a single axis (Fig. 2c, middle).
- **Fixed Joint:** A connection type implemented using PyBullet’s native `JOINT_FIXED` constraint type (Fig. 2c, bottom). This rigid connection completely eliminates all relative degrees of freedom between objects, preventing any relative motion. Fixed joints are particularly useful for creating structural stability and for temporarily immobilizing specific tiles during interactive simulations.

## 2.4 Force Models for Actuation and Dynamics

After constructing the kirigami tiles and their connections, we implement a physics-based deployment simulation. The dynamic behavior of the kirigami structure is governed by various configurable force models, including simple expansion forces for basic radial deployment and more advanced target-based actuation.

**Center-of-Mass Expansion Forces** For basic radial expansion of kirigami structures, PyKirigami provides an automatic expansion mode that applies forces to each tile’s center of mass, directing them outward from the structure’s global center. This method is particularly useful when precise target positions are not specified, serving as a fallback or simplified actuation approach.

**Target-Based Deployment Forces** While simple radial expansion can be achieved using center-of-mass forces described above, more complex deployments require a more sophisticated approach. Our simulator implements a vertex-based target model that provides precise control over the deployment process. In this model, each vertex of each tile is assigned a target position, and forces are applied to guide the vertices toward these targets. This approach allows for much more complex and controlled shape transformations than methods based solely on central forces or global expansion.

The deployment process is implemented through Algorithm 2, which calculates and applies appropriate forces and torques to achieve the desired configuration:

---

**Algorithm 2** Vertex-Based Target Force Application

---

- 1: **Input:** Body IDs and local coordinates from Algorithm 1, target vertex positions  $\{\tilde{v}_{i,j}\}$ , spring stiffness  $k_s$  and damping coefficient  $\mu_v$
  - 2: **for** each body representing tile  $\mathcal{T}_i$  **do**
  - 3:   Retrieve current position, orientation from the Bullet engine.
  - 4:   Transform local vertex coordinates to world coordinates.
  - 5:   Initialize net force  $\mathbf{F}_i = \mathbf{0}$  and net torque  $\boldsymbol{\tau}_i = \mathbf{0}$ .
  - 6:   **for** each vertex  $j$  in tile  $i$  **do**
  - 7:     Compute vertex force  $\mathbf{f}_{i,j} = k_s(\tilde{v}_{i,j} - v_{i,j})$ .
  - 8:     Add to net force:  $\mathbf{F}_i += \mathbf{f}_{i,j}$
  - 9:     Compute moment arm  $\mathbf{r}_{i,j} = v_{i,j} - \mathbf{c}_i$ .
  - 10:    Add to net torque:  $\boldsymbol{\tau}_i += \mathbf{r}_{i,j} \times \mathbf{f}_{i,j}$ .
  - 11:   **end for**
  - 12:   Apply net force  $\mathbf{F}_i - \mu_v \cdot \mathbf{v}_i$  and torque  $\boldsymbol{\tau}_i$  to tile  $\mathcal{T}_i$ .
  - 13: **end for**
- 

This vertex-based approach offers several advantages over simpler force models, including precise shape control, natural rotational behavior, and the ability to follow complex deployment paths.

**Environmental and Stabilization Forces** Beyond the actuation forces, PyKirigami models key environmental effects and stabilization mechanisms, which are fully configurable by the user to simulate diverse physical scenarios:

- **Gravitational Loading:** The magnitude and direction of the gravity vector can be specified to model deployment under various load conditions.

- **Numerical Damping:** To enhance stability and simulate energy dissipation, the model includes two configurable damping mechanisms. First, tunable linear and angular damping coefficients are applied to each rigid body to dissipate system-wide kinetic energy and ensure stable convergence to quasi-static equilibrium. Second, the actuation forces incorporate a damping factor (as seen in Algorithm 2) to promote smooth and stable deployment dynamics.
- **Contact Modeling:** The simulator supports interactions with external surfaces, such as a configurable ground plane, and models the resulting collision and friction forces.

## 3 Results

### 3.1 2D and 3D Deployment Simulations

To demonstrate the versatility and effectiveness of PyKirigami, we present a curated set of examples grouped by deployment dimensionality. These cases showcase how the simulator’s automated deployment mechanisms, environmental controls, and interactive features are applied to solve distinct challenges in 2D and 3D kirigami systems. For detailed simulation parameters and per-example configurations, see Appendix C. See also Supplementary Video S1–S4 for the videos of the deployment process of various 2D and 3D kirigami examples.

#### 3.1.1 2D Deployments and Interactive Morphing

Planar kirigami systems often involve in-plane expansion or complex shape-morphing between multiple stable states. We demonstrate PyKirigami’s capabilities for these scenarios with two distinct examples.

First, we consider the 2D expansion of the square-to-circle kirigami structure from [18] as shown in Fig. 3a. This example highlights the use of the basic Center-of-Mass Expansion Forces for straightforward radial deployment. More importantly, it demonstrates the essential role of Environmental and Stabilization Forces. By enabling a ground plane (Contact Modeling) and a downward gravity vector (Gravitational Loading), the deployment is constrained to the XY-plane, effectively simulating deployment on a physical surface and preventing the out-of-plane buckling that would otherwise occur in such a flexible structure.

Second, we showcase a compact reconfigurable kirigami model from [25], which has multiple closed and compact contracted states (see Fig. 3b). Unlike the open deployment in panel a, this transition involves strong hinge rotations, contact, and friction, and is sensitive to dissipation and control. We therefore analyze its passive dynamics (implicit hinge elasticity) and show how to achieve stable, deterministic deployment via target-based actuation in the next subsection.

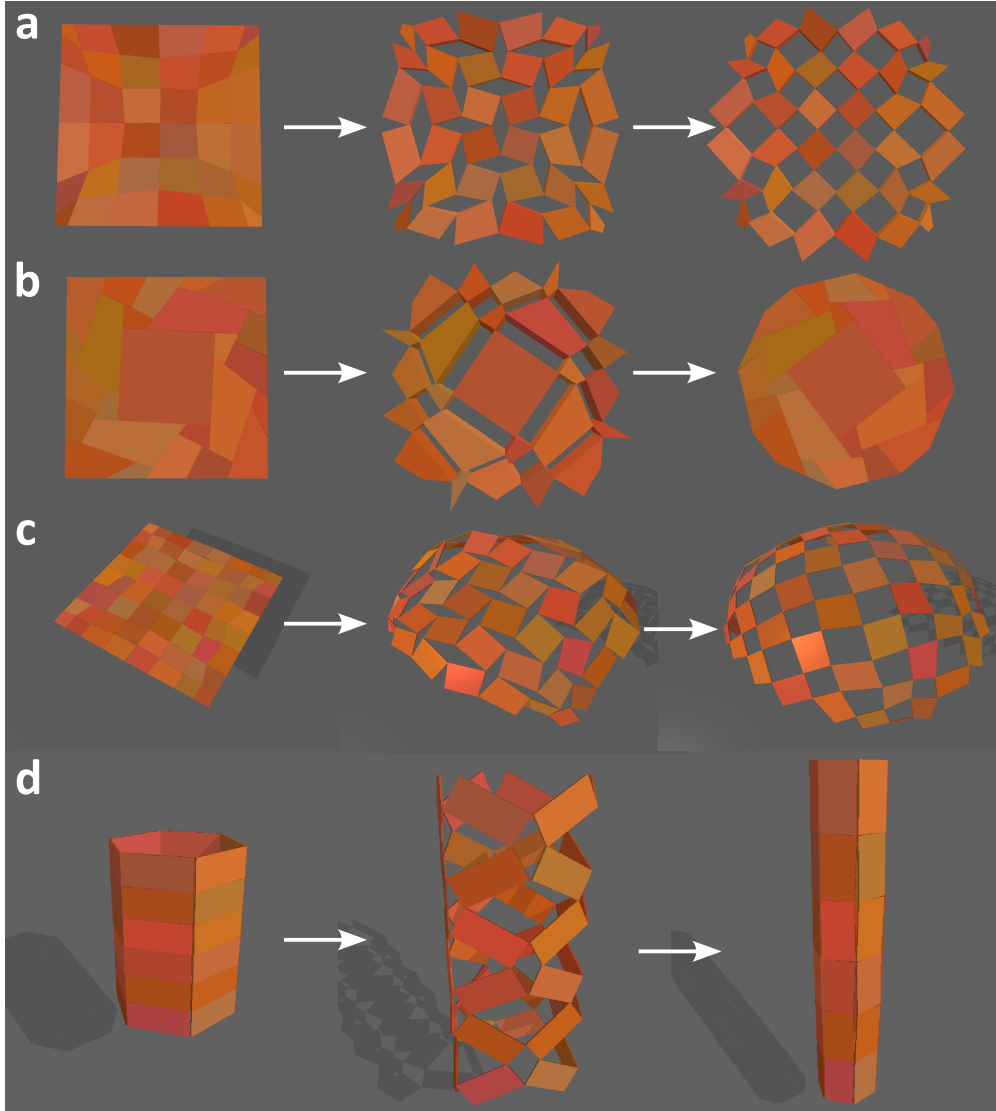


Figure 3: **Examples of 2D and 3D kirigami deployment achieved by PyKirigami.** **a**, The 2D deployment of the square-to-circle kirigami structure achieved by PyKirigami with automated radial expansion, stabilized by environmental forces. **b**, The 2D deployment of the compact reconfigurable kirigami model produced by PyKirigami. **c**, The 2D-to-3D deployment of the square-to-spherical-cap kirigami model achieved by PyKirigami, driven by the target-based force algorithm. **d**, The 3D-to-3D deployment and reconfiguration of the cylinder kirigami model achieved by PyKirigami, showcasing volumetric shape control.

### 3.1.2 3D Deployments and Volumetric Transformations

The transformation from flat sheets to 3D surfaces, or between different 3D configurations, represents a significant challenge in kirigami simulation. Our next examples demonstrate how PyKirigami addresses these complex, out-of-plane dynamics.

The 2D-to-3D deployment of a square-to-spherical-cap kirigami model shown in Fig. 3c exemplifies the necessity of the Target-Based Deployment Forces (Algorithm 2). Simple expansion or manual interaction is insufficient to control the complex, coupled bending and stretching deformations required for this transformation. The vertex-based target model provides the precise control needed to guide the structure through its out-of-plane path, ensuring stable convergence to the desired spherical geometry. This case also underscores the importance of parameter tuning, where the actuation spring stiffness ( $k_s$ ) and damping ( $\mu$ ) are calibrated to balance deployment speed with stability.

Finally, we demonstrate a 3D-to-3D deployment with a compact reconfigurable cylinder kirigami structure as shown in Fig. 3d. This highlights the robustness of the Target-Based Deployment Forces for guiding complex, non-radial paths in three dimensions. Actuating the structure from a compact, folded state to its fully deployed form requires targets that define not just a final shape, but a collision-free volumetric transformation. This proves the model’s suitability for simulating advanced systems like deployable space structures or reconfigurable robotics.

For completeness, while all examples in Fig. 3 use automated actuation (radial or target-based forces applied each simulation step), PyKirigami also supports a no-force mode and fully interactive runs in the GUI (manual actuation, pin/unpin, pause/reset). In Appendix C, we show how to apply these functionalities to achieve the target shape of Fig. 3b.

## 3.2 Geometric Fidelity of Deployment

PyKirigami utilizes a maximal-coordinate formulation where joint closures are enforced via an impulse-based solver (Projected Gauss-Seidel). Unlike reduced-coordinate approaches that strictly enforce kinematic loops, this iterative method inherently permits constraint violations (drift) between connected vertices. To rigorously assess the impact of this numerical relaxation on kinematic accuracy, we perform a quantitative validation on two distinct kirigami structures: a parametric rectangular tessellation kirigami structure and a complex square-to-disk kirigami structure. In both cases, the simulated deployment trajectories are compared directly against exact analytical solutions derived from the geometric design parameters.

### 3.2.1 Benchmark Case 1: Rectangular Tessellation

We first consider a standard  $M \times N$  rectangular tessellation kirigami structure with deployment angle  $\theta$  as a benchmark. The theoretical vertex position  $p_i^{\text{th}}$  at  $\theta$  can be derived easily (see Appendix D). We initialize a  $4 \times 4$  grid in PyKirigami and actuate it from  $\theta = 0$  to  $\theta = \pi/2$ . At each time step, we quantify the drift by computing the Euclidean error  $\|p_i^{\text{sim}} - p_i^{\text{th}}\|$  for all vertices  $i$ .

As shown in Fig. 4, the error profile demonstrates the high fidelity of the impulse-based solver. The simulation initializes with a transient spike in maximum deviation 2.5% as the solver resolves the ill-conditioned constraints near the compact state. Crucially, the mean relative error remains exceptionally low throughout the entire deployment process. This confirms that the transient spike is isolated to a few specific tiles and joints and does not propagate

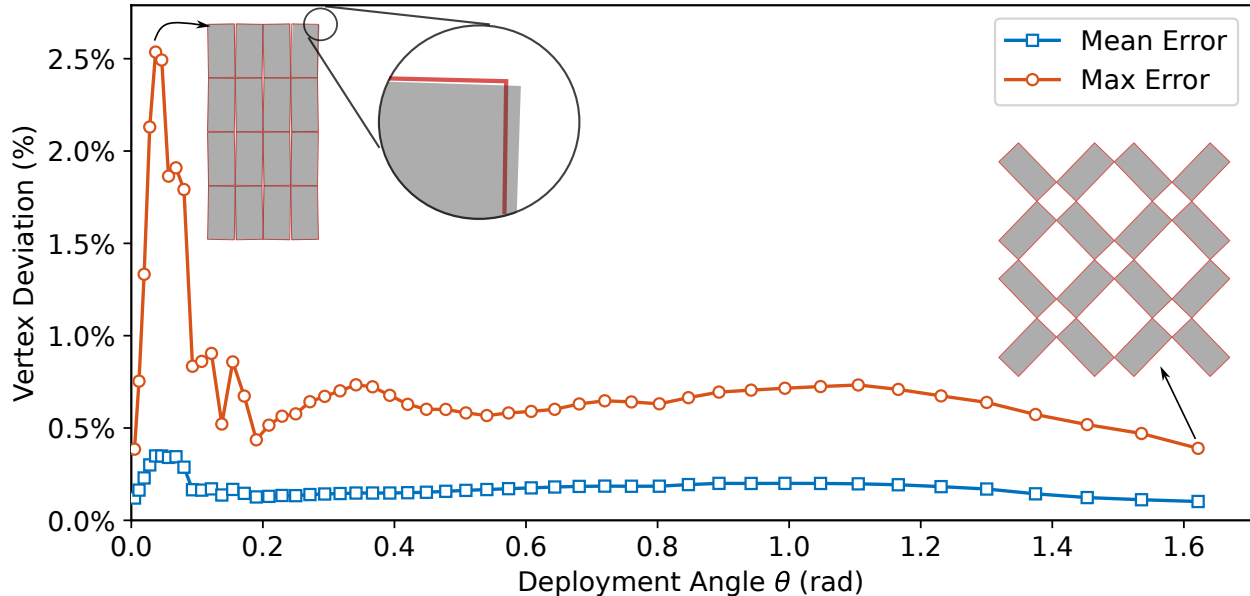


Figure 4: **Quantitative validation of PyKirigami using the rectangular tessellation kirigami structure.** The plot shows the maximal and mean vertex error versus the deployment angle  $\theta$ . Insets show a comparison of the simulated geometry (gray solid) against the theoretical trajectory (red wireframe) at two points. The left inset shows tessellation at the maximum deviation ( $\theta \approx 0.04$ ) with the magnified view highlighting the drift. The right inset displays the fully deployed state, in which the error is negligible.

through the system. The negligible mean error demonstrates that PyKirigami maintains vertex-level coherence, verifying the implementation of the topology constraint.

### 3.2.2 Benchmark Case 2: Square-to-disk Structure

Having validated the solver’s precision on the above benchmark case, we consider analyzing the deployment of the more complex square-to-disk structure as shown in Fig. 3b. As explained in the theoretical construction of the structure in [25], the deployment of it is also a single-degree-of-freedom mechanism (see Appendix D) where the global radius  $R$  is a deterministic function of the tile rotation angle  $\theta$ . Therefore, in Fig. 5 we plot the global radius against the local deployment angle obtained by Pykirigami and compare the result with the analytical result in [25], from which we can see that the discrete data samples obtained by PyKirigami at different time points of the deployment (red circles) show excellent agreement with the theoretical curve  $R(\theta)$  (blue solid line). While micro-deviations exist at the hinge level (drift), the global topology remains locked to the correct deployment path, validating the tool for macroscopic shape analysis.

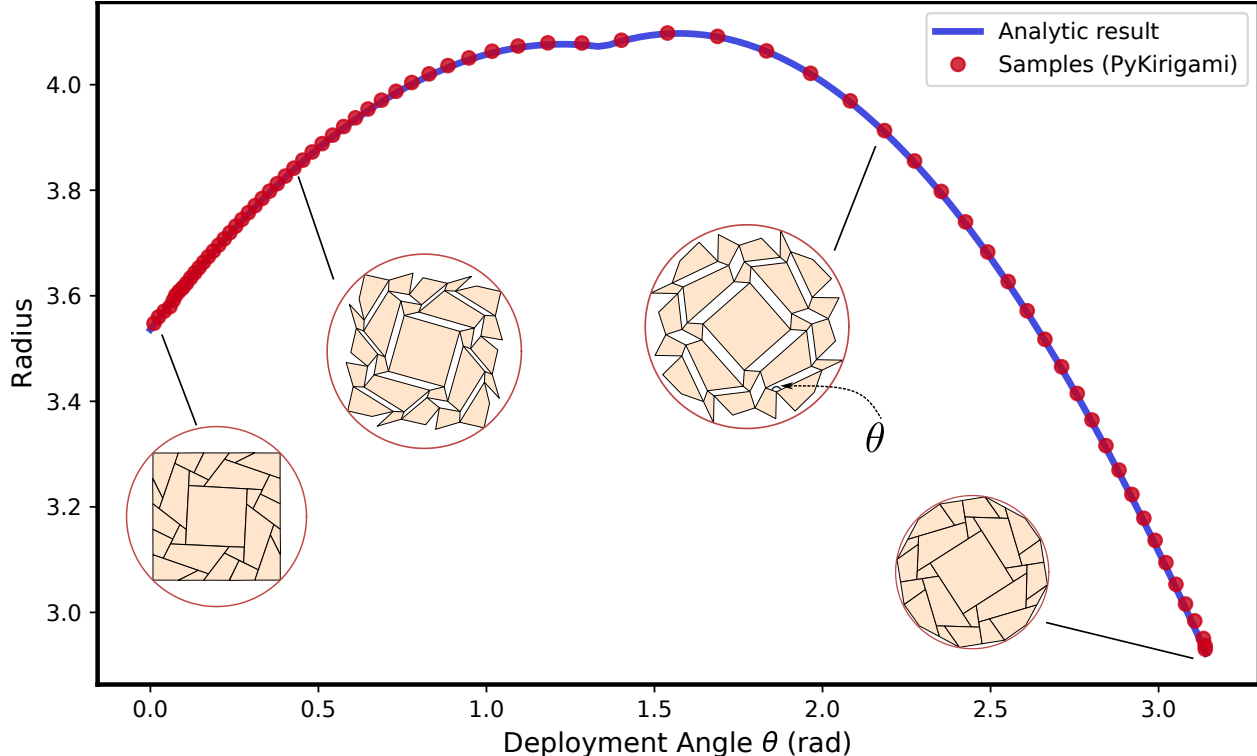


Figure 5: **Quantitative validation of PyKirigami using the square-to-disk kirigami structure.** Here, we plot the global radius  $R$  versus the deployment angle  $\theta$  for both the simulations obtained by PyKirigami (red dots) and the analytical result by [25] (blue solid line). The PyKirigami simulation data align closely with the analytical prediction, confirming that the solver captures the correct kinematic mode. The insets show four snapshots from the simulation.

### 3.3 Actuation Tuning and Numerical Convergence

As demonstrated in the rectangular tessellation benchmark case (Fig. 4), the solver enforces finite collision margins at the joints, which behave like a repulsive contact force to prevent interpenetration. Consequently, the actuation mechanism must be carefully tuned. If the force is too weak, the structure “jams” prematurely, far from the physical limit. If the force is too strong, it fights the collision engine.

To quantify this operational window, we perform a parametric study of the stiffness  $k_s$  using the square-to-disk example. We target the fully compact disk state and vary the stiffness  $k_s \in \{50, 100, 1000\}$  while maintaining spring damping  $\mu_v = 8.5$ , environmental damping of 0.1 and ground friction of 0.5. The deployment dynamics are analyzed in Fig. 6.

- **Underactuated (Low Stiffness,  $k_s = 50$ , Fig. 6a):** As the structure approaches the compact state, the actuation force by spring is insufficient to overcome the cumulative resistance of ground friction and joint contact impulse. Consequently, the structure

jams in an intermediate state, failing to reach the physical packing limit. This highlights the necessity of a minimum actuation threshold to get the desired deployment.

- **Critically Actuated (Medium Stiffness,  $k_s = 100$ , Fig. 6b):** The actuation force is strong enough to compress the tiles against their collision boundaries, effectively closing the gaps to the solver’s limit. Simultaneously, the force is low enough that the system’s damping can dissipate the kinetic energy upon arrival. The structure converges rapidly to the target state and remains stable, demonstrating that PyKirigami can achieve maximal compaction without instability.
- **Overactuated (High Stiffness,  $k_s = 1000$ , Fig. 6c):** A very strong spring force causes the structure to rapidly accelerate towards the target. While it reaches the target configuration, the high influx of energy and the resulting high-velocity collisions induce a persistent “wobble” or chatter in the following state.

## 4 Discussion

In this work, we have developed PyKirigami, an efficient and open-source computational tool for the deployment simulation of kirigami structures. Specifically, we have demonstrated the ability of our PyKirigami simulator for handling different 2D and 3D kirigami structures with different customized settings in terms of the tile geometries, tile connections, and other deployment parameters. Altogether, our simulation tool can significantly facilitate the computational modelling process for kirigami structures, thereby paving a new way for the design of shape-morphing metamaterials.

While PyKirigami provides a robust framework for rigid-body dynamics, we acknowledge its current limitations. First, note that the simulator considers the 3D kirigami tiles and their connections without capturing material elasticity, plasticity, or fracture. Also, high-fidelity stress/strain analysis would still require FEA methods. Besides, the current implementation of the simulator assumes the preservation of the kirigami tile connections throughout the deployment, while real-time cutting or topology changes are not supported. Our simulator is therefore best positioned as a tool for rapid prototyping, kinematic analysis, and exploring the global deployment dynamics of complex kirigami assemblies.

**Data Availability** The code and data are available on GitHub at <https://github.com/andy-qhjiang/PyKirigami>.

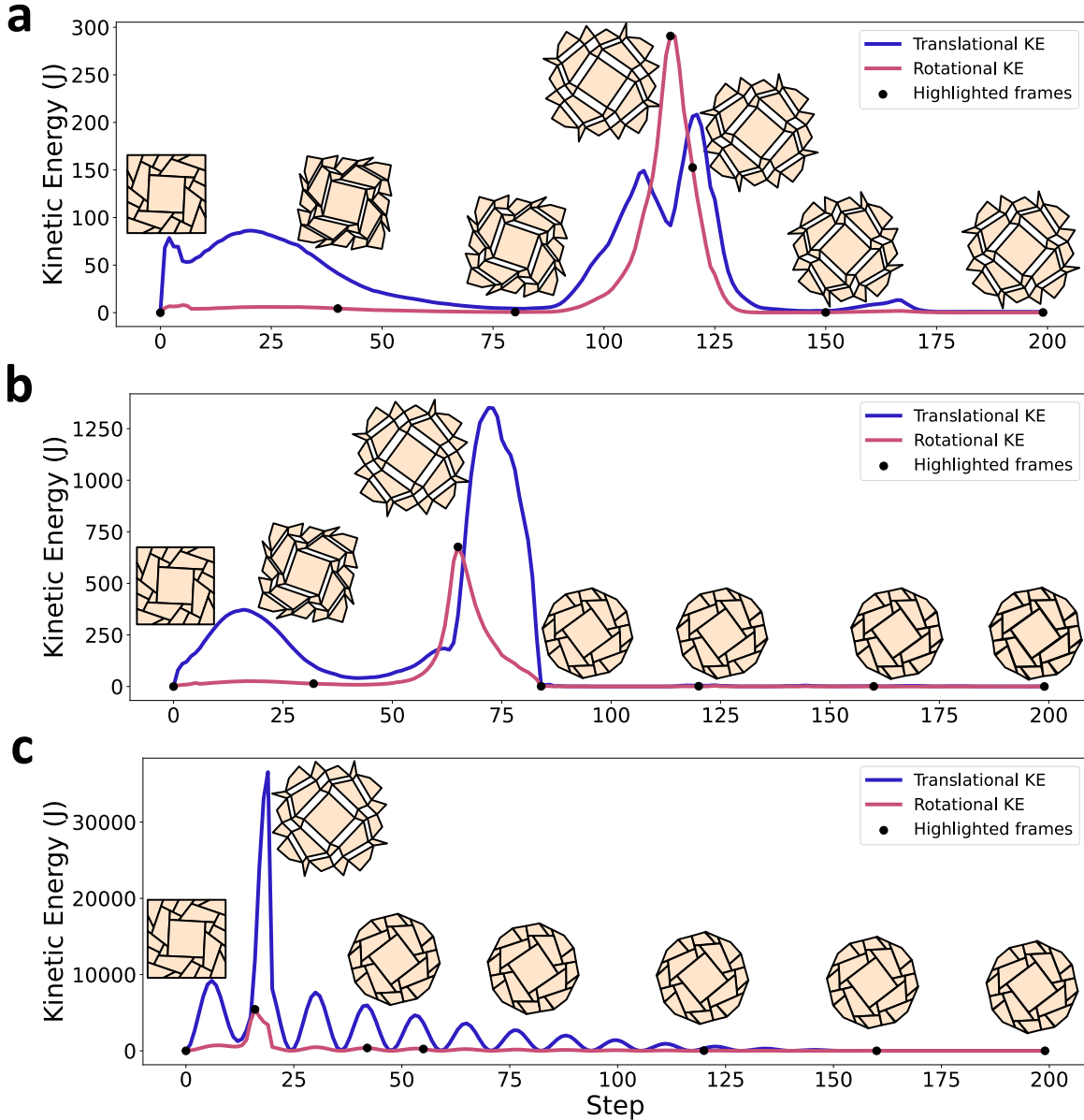


Figure 6: **Parametric study of active control for stabilizing the square-to-disk deployment.** The square-to-disk structure is driven toward the compact disk state under varying spring stiffness  $k_s$ . **a**, *Underactuated* ( $k_s = 50$ ): Weak spring forces are insufficient to overcome internal and environmental resistance, trapping the structure in an intermediate state. **b**, *Critically Actuated* ( $k_s = 100$ ): The actuation is sufficient to achieve the target configuration, where the structure stabilizes after a final self-collision. **c**, *Overactuated* ( $k_s = 1000$ ): Excessive stiffness causes a rapid deployment but induces persistent, high-frequency oscillations (chatter) around the target state, preventing full stabilization.

## References

- [1] E. Barchiesi, M. Spagnuolo, L. Placidi, Mechanical metamaterials: a state of the art, *Math. Mech. Solids* 24 (1) (2019) 212–234.
- [2] Z. Zhai, L. Wu, H. Jiang, Mechanical metamaterials based on origami and kirigami, *Appl. Phys. Rev.* 8 (4) (2021).
- [3] X. Li, W. Peng, W. Wu, J. Xiong, Y. Lu, Auxetic mechanical metamaterials: from soft to stiff, *Int. J. Extreme Manuf.* 5 (4) (2023) 042003.
- [4] G. P. T. Choi, Computational design of art-inspired metamaterials, *Nat. Comput. Sci.* 4 (8) (2024) 549–552.
- [5] L. Jin, S. Yang, Engineering kirigami frameworks toward real-world applications, *Adv. Mater.* 36 (9) (2024) 2308560.
- [6] X. Dang, G. Paulino, Kirigami engineering: The interplay between geometry and mechanics, *Appl. Mech. Rev.* (2025) 1–21.
- [7] S. Jiang, X. Liu, J. Liu, D. Ye, Y. Duan, K. Li, Z. Yin, Y. Huang, Flexible metamaterial electronics, *Adv. Mater.* 34 (52) (2022) 2200070.
- [8] Z. Song, X. Wang, C. Lv, Y. An, M. Liang, T. Ma, D. He, Y.-J. Zheng, S.-Q. Huang, H. Yu, et al., Kirigami-based stretchable lithium-ion batteries, *Sci. Rep.* 5 (1) (2015) 10988.
- [9] Y. Yang, K. Vella, D. P. Holmes, Grasping with kirigami shells, *Sci. Robot.* 6 (54) (2021) eabd6426.
- [10] J. N. Grima, K. E. Evans, Auxetic behavior from rotating triangles, *J. Mater. Sci.* 41 (10) (2006) 3193–3196.
- [11] J. N. Grima, K. E. Evans, Auxetic behavior from rotating squares, *J. Mater. Sci. Lett.* 19 (2000) 1563–1565.
- [12] D. Attard, J. N. Grima, Auxetic behaviour from rotating rhombi, *Phys. Status Solidi B* 245 (11) (2008) 2395–2404.
- [13] A. Rafsanjani, D. Pasini, Bistable auxetic mechanical metamaterials inspired by ancient geometric motifs, *Extreme Mech. Lett.* 9 (2016) 291–296.
- [14] M. Stavric, A. Wiltsche, Geometrical elaboration of auxetic structures, *Nexus Netw. J.* 21 (2019) 79–90.
- [15] L. Liu, G. P. T. Choi, L. Mahadevan, Wallpaper group kirigami, *Proc. R. Soc. A* 477 (2252) (2021) 20210161.

- [16] L. Liu, G. P. T. Choi, L. Mahadevan, Quasicrystal kirigami, *Phys. Rev. Research* 4 (3) (2022) 033114.
- [17] B. G.-g. Chen, B. Liu, A. A. Evans, J. Paulose, I. Cohen, V. Vitelli, C. D. Santangelo, Topological mechanics of origami and kirigami, *Phys. Rev. Lett.* 116 (13) (2016) 135501.
- [18] G. P. T. Choi, L. H. Dudte, L. Mahadevan, Programming shape using kirigami tessellations, *Nat. Mater.* 18 (9) (2019) 999–1004.
- [19] S. Chen, G. P. T. Choi, L. Mahadevan, Deterministic and stochastic control of kirigami topology, *Proc. Natl. Acad. Sci.* 117 (9) (2020) 4511–4517.
- [20] G. P. T. Choi, L. H. Dudte, L. Mahadevan, Compact reconfigurable kirigami, *Phys. Rev. Research* 3 (4) (2021) 043030.
- [21] X. Dang, F. Feng, H. Duan, J. Wang, Theorem for the design of deployable kirigami tessellations with different topologies, *Phys. Rev. E* 104 (5) (2021) 055006.
- [22] Y. Zheng, I. Niloy, P. Celli, I. Tobasco, P. Plucinsky, Continuum field theory for the deformations of planar kirigami, *Phys. Rev. Lett.* 128 (20) (2022) 208003.
- [23] Y. Hong, Y. Chi, S. Wu, Y. Li, Y. Zhu, J. Yin, Boundary curvature guided programmable shape-morphing kirigami sheets, *Nat. Commun.* 13 (1) (2022) 530.
- [24] L. Wang, Y. Chang, S. Wu, R. R. Zhao, W. Chen, Physics-aware differentiable design of magnetically actuated kirigami for shape morphing, *Nat. Commun.* 14 (1) (2023) 8516.
- [25] L. H. Dudte, G. P. T. Choi, K. P. Becker, L. Mahadevan, An additive framework for kirigami design, *Nat. Comput. Sci.* 3 (5) (2023) 443–454.
- [26] C. Qiao, S. Chen, Y. Chen, Z. Zhou, W. Jiang, Q. Wang, X. Tian, D. Pasini, Inverse design of kirigami through shape programming of rotating units, *Phys. Rev. Lett.* 134 (17) (2025) 176103.
- [27] D. M. Sussman, Y. Cho, T. Castle, X. Gong, E. Jung, S. Yang, R. D. Kamien, Algorithmic lattice kirigami: A route to pluripotent materials, *Proc. Natl. Acad. Sci.* 112 (24) (2015) 7449–7453.
- [28] M. Konaković, K. Crane, B. Deng, S. Bouaziz, D. Piker, M. Pauly, Beyond developable: computational design and fabrication with auxetic materials, *ACM Trans. Graph.* 35 (4) (2016) 1–11.
- [29] M. Konaković-Luković, J. Panetta, K. Crane, M. Pauly, Rapid deployment of curved surfaces via programmable auxetics, *ACM Trans. Graph.* 37 (4) (2018) 1–13.
- [30] X. Wang, S. D. Guest, R. D. Kamien, Keeping it together: interleaved kirigami extension assembly, *Phys. Rev. X* 10 (1) (2020) 011013.

- [31] T. Chen, J. Panetta, M. Schnaubelt, M. Pauly, Bistable auxetic surface structures, *ACM Trans. Graph.* 40 (4) (2021) 1–9.
- [32] X. Dang, F. Feng, H. Duan, J. Wang, Theorem on the compatibility of spherical kirigami tessellations, *Phys. Rev. Lett.* 128 (3) (2022) 035501.
- [33] Y. Li, Q. Zhang, Y. Hong, J. Yin, 3D transformable modular kirigami based programmable metamaterials, *Adv. Funct. Mater.* 31 (43) (2021) 2105641.
- [34] X. Dang, S. Chen, A. E. Acha, L. Wu, D. Pasini, Shape and topology morphing of closed surfaces integrating origami and kirigami, *Sci. Adv.* 11 (18) (2025) eads5659.
- [35] L. Jin, A. E. Forte, B. Deng, A. Rafsanjani, K. Bertoldi, Kirigami-inspired inflatables with programmable shapes, *Adv. Mater.* 32 (33) (2020) 2001863.
- [36] N. An, A. G. Domel, J. Zhou, A. Rafsanjani, K. Bertoldi, Programmable hierarchical kirigami, *Adv. Funct. Mater.* 30 (6) (2020) 1906711.
- [37] R. Zhu, H. Yasuda, G. L. Huang, J. K. Yang, Kirigami-based elastic metamaterials with anisotropic mass density for subwavelength flexural wave control, *Sci. Rep.* 8 (1) (2018) 483.
- [38] N. A. Alderete, L. Medina, L. Lamberti, C. Sciammarella, H. D. Espinosa, Programmable 3D structures via kirigami engineering and controlled stretching, *Extreme Mech. Lett.* 43 (2021) 101146.
- [39] X. Ying, D. Fernando, M. A. Dias, Inverse design of programmable shape-morphing kirigami structures, *Int. J. Mech. Sci.* 286 (2025) 109840.
- [40] E. Coumans, Y. Bai, PyBullet, a Python module for physics simulation for games, robotics and machine learning, <http://pybullet.org> (2016).

# Appendix

## A Overview

PyKirigami is an open-source Python toolbox for simulating the 2D and 3D deployment of general kirigami structures. The simulator utilizes the PyBullet physics engine and is capable of simulating 2D-to-2D, 2D-to-3D, and 3D-to-3D kirigami deployments with interactive controls. The toolbox is freely available on GitHub:

<https://github.com/andy-qhjiang/PyKirigami>

The detailed installation instructions, usages, and example projects can be found in the user manual:

<https://github.com/andy-qhjiang/PyKirigami/wiki/Manual>

In this supplementary document, we focus on how we realize the key features and functionalities of PyKirigami to make it easy to be understood and extended by interested users.

## B Implementation Walkthrough

### B.1 Coordinate System Management

A fundamental concept in PyBullet, and 3D simulations in general, is the distinction between **world coordinates** and **local coordinates**. Understanding this is key to efficiently defining connections and analyzing the kirigami structure's motion.

**Frames and notation.** We first define the following:

- World frame: The fixed global frame.
- Local (base) frames: one per tile, with origins at the tile centers  $O_1$  (tile A) and  $O_2$  (tile B).
- Rotations:  $R_1, R_2 \in \text{SO}(3)$  map local coordinates to world for tiles A and B.
- Coordinates:  $\mathbf{p}_l$  and  $\mathbf{q}_l$  are the local coordinates of  $P$  and  $Q$ ;  $\mathbf{p}_w$  and  $\mathbf{q}_w$  are the corresponding world coordinates.

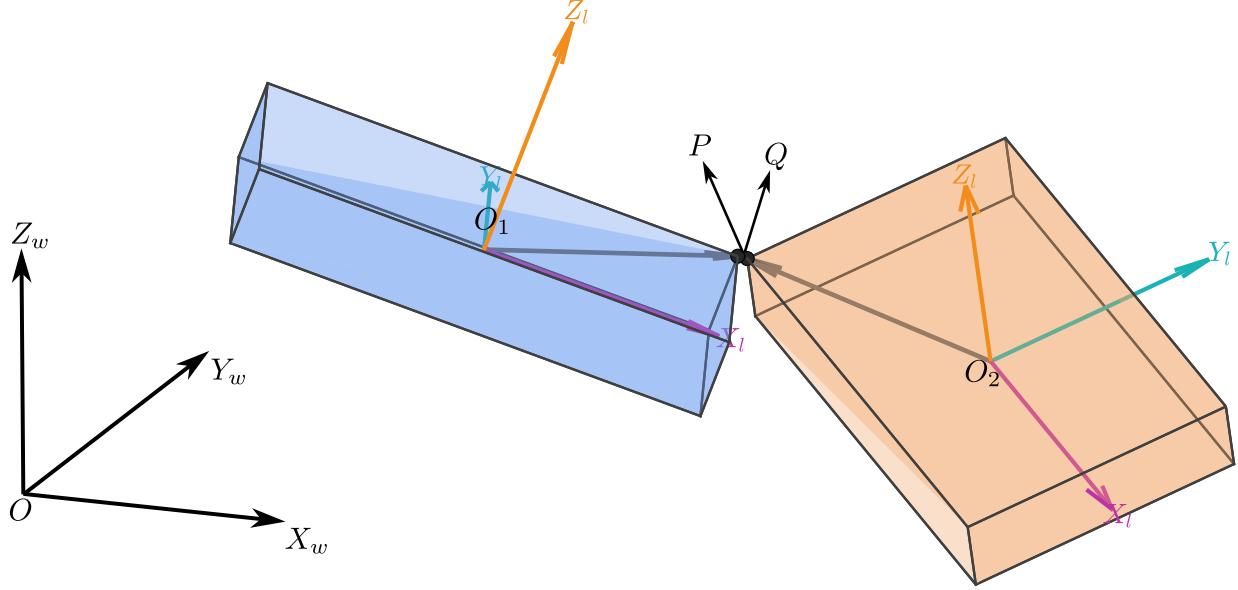


Figure 7: **Coordinate systems in PyBullet.** The fixed global axes  $(X_w, Y_w, Z_w)$  define the world coordinate system. Each kirigami tile (represented by a box) has its own local coordinate system  $(X_l, Y_l, Z_l)$  attached to its center. A corner vertex of the blue box, such as  $P$ , has constant local coordinates  $\mathbf{p}_l = P - O_1$  in its body’s frame, but its world coordinates  $\mathbf{p}_w$  change as the body moves.

**Local-world transforms.** The exact mappings are

$$\mathbf{p}_w = R_1 \mathbf{p}_l + O_1, \quad \mathbf{q}_w = R_2 \mathbf{q}_l + O_2, \quad (2)$$

and, inversely,

$$\mathbf{p}_l = R_1^\top (\mathbf{p}_w - O_1), \quad \mathbf{q}_l = R_2^\top (\mathbf{q}_w - O_2). \quad (3)$$

See Fig. 7 for an illustration. For convenience, we provide helper functions that implement the local-world transforms:

```
import pybullet as p
import numpy as np

def local_to_world(body_id, p_local):
    pos, orn = p.getBasePositionAndOrientation(body_id)
    # pos is the world frame position of tile center O_i
    R = np.array(p.getMatrixFromQuaternion(orn)).reshape(3, 3) # R_i
    return (R @ np.asarray(p_local)) + np.asarray(pos)

def world_to_local(body_id, p_world):
    pos, orn = p.getBasePositionAndOrientation(body_id)
    R = np.array(p.getMatrixFromQuaternion(orn)).reshape(3, 3)
    return (R.T @ (np.asarray(p_world) - np.asarray(pos)))
```

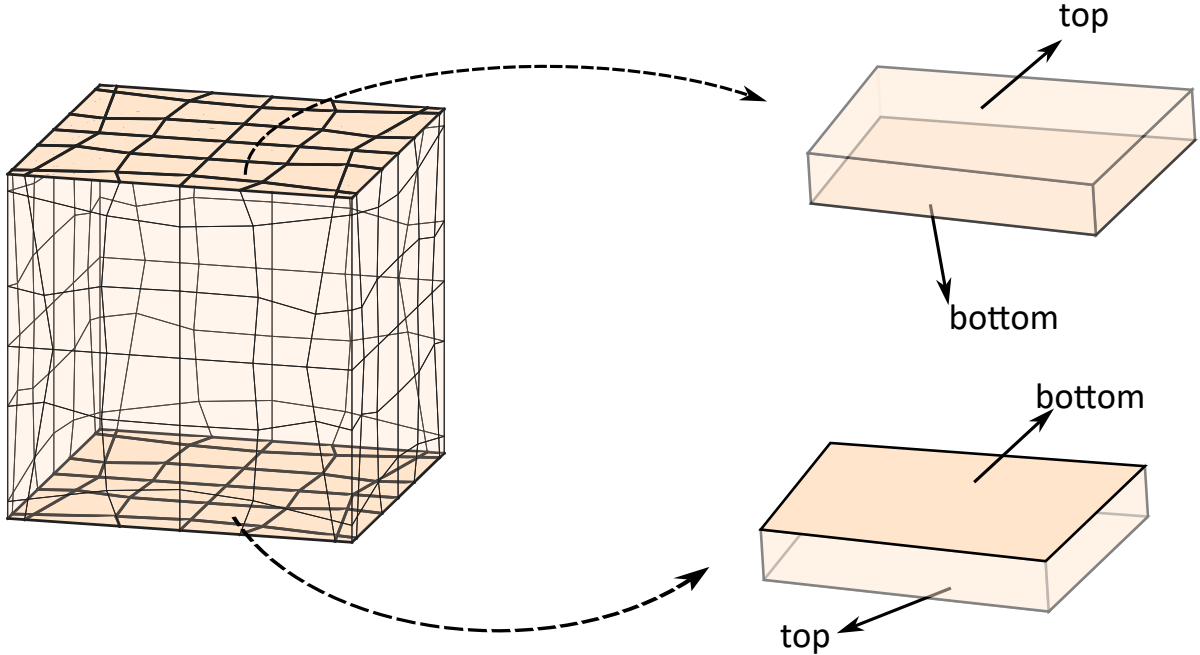


Figure 8: **An illustration of face extrusion for 3D kirigami structures.** Here, note that the quadrilateral patches on opposite faces of the cube are congruent, but their orientations are different. As the outward normal flips ( $\mathbf{n} \mapsto -\mathbf{n}$ ), the vertex order must be reversed to maintain outward-facing normals. If the top face uses  $(v_0, v_1, v_2, v_3)$  in counter-clockwise order (viewed from outside), the corresponding bottom face should be indexed  $(v_0, v_3, v_2, v_1)$ .

## B.2 Object Creation in PyBullet

Given the planar vertices of a tile in world coordinates, we construct a 3D “brick” of thickness  $t$ . The core of this process is to create two distinct geometric representations for the tile, both defined in its local (base) frame: a simple **collision shape** for physics calculations and a detailed **visual shape** for rendering. This separation optimizes performance while ensuring visual fidelity.

**Extrusion and face orientation.** As described in the main text (see also main text Fig. 2), we define the tile’s outward unit normal  $\mathbf{n}$  in world coordinates and extrude along  $+\mathbf{n}$  to obtain the top face, while the original tile becomes the bottom face. In Fig. 8, we further illustrate this idea for 3D kirigami structures. Specifically, this local-normal convention is essential in 3D-to-3D deployments, where the world  $z$ -axis generally does not align with the tiles normal.

**Collision Shape Construction.** The collision shape is used by the physics engine to detect contact, resolve forces, and simulate dynamics. For stability and speed, we set it as a simple convex volume since this already meets our requirements for the simulation. After

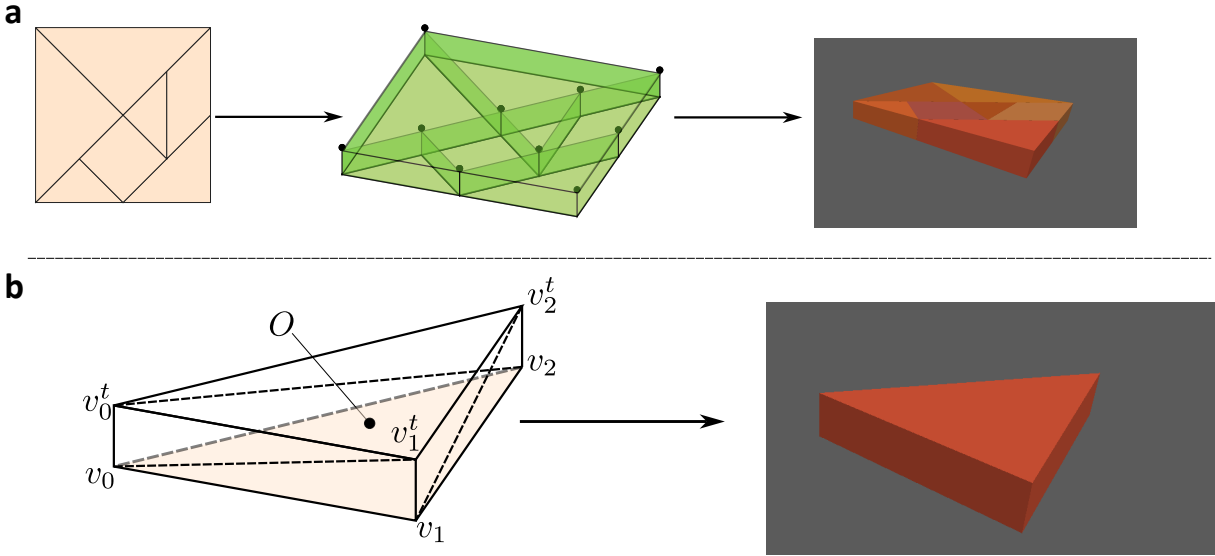


Figure 9: **Brick creation in the local frame.** **a**, Extrusion: We compute the world-space top vertices  $v_j^t = v_j + t \cdot \mathbf{n}$  and the base origin  $O$  (tile center), then convert both bottom and top vertices to local coordinates via  $u_j = v_j - O$  and  $u_j^t = v_j^t - O$ . **b**, Mesh construction: We build a convex collision vertex cloud (local) and a per-vertex-normal visual mesh (local) with cap and side faces.

extrusion, we pass the list of local coordinates

$$\{u_j = v_j - O, u_j^t = v_j^t - O\}$$

to `p.createCollisionShape`. PyBullet automatically computes the convex hull of the vertices to form a robust and efficient, though invisible, collision mesh (Fig. 9). Below is an example of the collision shape creation for a triangular tile:

```

# PyBullet computes the convex hull based on local coordinates
# which is exactly the triangular prism
col_shape = p.createCollisionShape(
    shapeType=p.GEOM_MESH,
    vertices=[
        [x1, y1, z1], # coordinates of u0
        [x2, y2, z2], # coordinates of u1
        [x3, y3, z3], # coordinates of u2
        [x4, y4, z4], # coordinates of u0t
        [x5, y5, z5], # coordinates of u1t
        [x6, y6, z6], # coordinates of u2t
    ]
)

```

**Visual Shape Construction.** The visual shape provides a detailed mesh for rendering sharp edges and correct lighting. The key to achieving this is understanding that PyBullet’s

graphics API assigns normals on a **per-vertex** basis. To create flat-shaded faces with hard edges, we must often duplicate geometric vertices in our data buffers, pairing each copy with the correct face normal. We illustrate this by building a single rectangular side face of the brick illustrated in Fig. 9b, defined by local bottom vertices  $(u_0, u_1)$  and top vertices  $(u_0^t, u_1^t)$ . Below is an example:

```
# Define the 4 unique vertices of the rectangular face
vis_vertices = [
    u0, # index 0
    u1, # index 1
    u1t, # index 2
    u0t # index 3
]

# The API requires one normal per vertex. Identical For a flat face.
n_side = calculate_face_normal(v0, v1, v1t)
vis_normals = [n_side]*len(vis_vertices)

# Define two triangles using indices into the vertex/normal lists
vis_indices = [
    0, 1, 2, # First triangle: (v0, v1, v1t)
    0, 2, 3 # Second triangle: (v0, v1t, v0t)
]

# These lists are passed to create the visual component of the body
vis_shape = p.createVisualShape(
    shapeType=p.GEOM_MESH,
    vertices=vis_vertices,
    indices=vis_indices,
    normals=vis_normals,
    rgbaColor=[...],
    specularColor=[0.8, 0.8, 0.8] # Glare; smaller is less shiny
)
```

**Visual customization.** The tile’s appearance can be modified at creation time or dynamically via the `rgbaColor` parameter. We use sky blue color as an indicator of fixing an object during simulation:

```
p.changeVisualShape(bodyUniqueID=body_id, rgbaColor=[0.53, 0.81, 0.92, 1.0
])
```

**Assembly.** With both shapes defined in the local frame, instantiating the rigid body is straightforward. The only world quantity to be supplied is the base pose  $(O, R)$ ; typically  $R = I$  at load time.

```
def create_brick_body(col_shape, vis_shape, base_origin_world, mass=1.0,
                    base_quat=[0,0,0,1]):
    return p.createMultiBody(
        baseMass=mass,
```

```

        baseCollisionShapeIndex=col_shape,
        baseVisualShapeIndex=vis_shape,
        basePosition=base_origin_world, # world position of local
                                         origin
        baseOrientation=base_quat # usually identity; optional
    )

```

This completes the brick creation pipeline: (i) extrude and define local geometry, (ii) build a convex collision shape and a flat-shaded visual mesh with per-vertex normals via vertex duplication, and (iii) instantiate the rigid body at its world pose.

### B.3 Creating Inter-Tile Constraints

With each tile defined as a rigid body in its own local frame, we now connect them to form the kirigami structure. PyKirigami uses PyBullet’s constraint system to model the joints between tiles. All constraints are defined by specifying pivot points in the **local coordinates** of the connected bodies, leveraging the framework established in the previous sections.

**Constraint Validation.** Before creating any physics objects, it is crucial to validate that the provided vertex and constraint data are consistent. For a kirigami structure to be physically valid, the world-space positions of any two vertices designated as a pivot pair must coincide. PyKirigami performs this check before entering the simulation loop:

```

def validate_constraints(vertices, constraints, tolerance=1e-6):
    # Unpack constraint data (e.g., for a spherical joint)
    for i, constraint in enumerate(constraints):
        f1, v1, f2, v2 = constraint[:4]
        # Get vertex positions for constraint endpoints
        p1_world = np.array(vertices[f1][3*v1:3*v1+3])
        p2_world = np.array(vertices[f2][3*v2:3*v2+3])
        # Check distance
        dist = np.linalg.norm(np.array(p1_world) - np.array(p2_world))
        if dist > tolerance:
            raise ValueError(f"Constraint validation failed: distance is {
                               dist}")

```

**Spherical Joint.** As illustrated in Fig. 7, a connection is defined by a pair of pivot points, such as  $P$  on tile A and  $Q$  on tile B. We provide PyBullet with the constant local coordinates of these pivots,  $\mathbf{p}_l$  and  $\mathbf{q}_l$ . The physics engine then ensures that the world-space positions of these points,  $\mathbf{p}_w$  and  $\mathbf{q}_w$ , satisfy the constraint equation

$$R_1 \cdot \mathbf{p}_l + O_1 = R_2 \cdot \mathbf{q}_l + O_2, \quad (4)$$

at every time step. It is implemented with a single JOINT\_POINT2POINT constraint as follows:

```

# create spherical joint and return cid (constraint ID)
def connect_spherical(bodyA, bodyB, pA_local, pB_local):

```

```

return p.createConstraint(
    parentBodyUniqueId=bodyA,
    parentLinkIndex=-1,
    childBodyUniqueId=bodyB,
    childLinkIndex=-1,
    jointType=p.JOINT_POINT2POINT,
    jointAxis=[0,0,0],
    parentFramePosition=pA_local,
    childFramePosition=pB_local
)

```

Since the kirigami bricks have thickness, we must specify whether a pivot lies on the bottom face (original vertices) or the top face (extruded vertices) as illustrated in the main text. Our constraint file format supports an optional face specifier  $\mathfrak{t}$  (1 for bottom, 2 for top). When parsing, we select the appropriate local vertex vector, either  $\mathbf{u}_j$  (bottom) or  $\mathbf{u}_j^t$  (top), to use as the pivot.

**Hinge Joint.** A hinge restricts rotation to a single axis, providing one rotational degree of freedom. In PyKirigami, we robustly implement a hinge by using **two** non-coincident spherical joints. The line connecting the two pivot pairs defines the hinge axis. This method is numerically stable and works well for bodies with finite thickness:

```

def connect_hinge(bodyA, bodyB, pA1, pB1, pA2, pB2):
    cid1 = connect_spherical(bodyA, bodyB, pA1, pB1)
    cid2 = connect_spherical(bodyA, bodyB, pA2, pB2)
    return [cid1, cid2]

```

**Fixed Joint.** This joint removes all six relative degrees of freedom between two bodies, effectively welding them together. We use the native JOINT\_FIXED constraint. This is particularly useful for anchoring a tile to the world (by constraining it to a static body) or for creating rigid composite structures:

```

def fix_object_to_world(body_id):
    pos, orn = p.getBasePositionAndOrientation(body_id)
    constraint_id = p.createConstraint(
        parentBodyUniqueId=body_id,
        parentLinkIndex=-1,
        childBodyUniqueId=-1, # World frame
        childLinkIndex=-1,
        jointType=p.JOINT_FIXED,
        jointAxis=[0, 0, 0],
        parentFramePosition=[0, 0, 0],
        childFramePosition=pos, # tile center 0_i in world
        parentFrameOrientation=[0, 0, 0, 1],
        childFrameOrientation=orn # tile orientation in world
    )
    p.changeConstraint(cid, maxForce=max_force)
    return cid

```

**Remark.** To make a body immovable, one could either use a `JOINT_FIXED` constraint or set the body’s mass to zero. For an articulated system like a kirigami structure, the constraint-based approach is recommended since an anchored tile must still be able to transmit forces and torques from the rest of the structure to the world. A fixed joint allows for this, as the body remains a dynamic participant in the simulation. In contrast, setting a body’s mass to zero removes it from the dynamics calculation, which can cause solver instability when other dynamic bodies are joined to it. The practice of setting mass to zero is best reserved for defining permanent, static environment geometry like floors or immovable obstacles.

## B.4 Interactive Control and Simulation State Management

The runtime system comprises three layers:

- Entry point and GUI loop (`run_sim.py`)
- Simulation (initialization and force selection)
- Controllers: `SimulationController` (runtime stepping/state) and `InteractionController` (`pin/unpin`, snapshots, and save data)

**Simulation: initialization and force selection.** The `Simulation` class constructs all rigid bodies and constraints from files, configures damping/environment, and prepares data for runtime control. It returns a dictionary `simulation_data` for downstream controllers, summarized in Table 1.

Table 1: Contents of the `simulation_data` dictionary passed to controllers.

Key	Description
<code>args</code>	Parsed command-line configuration (timestep, damping, thickness, modes, etc.).
<code>bricks</code>	List of PyBullet body IDs (one per tile).
<code>local_coords</code>	Bottom-face local vertex coordinates per tile (used for local-to-world transforms during runtime).
<code>constraint_ids</code>	List of PyBullet constraint IDs created between tiles.
<code>visual_mesh</code>	List of visual mesh for each tile to be exported as an OBJ file.
<code>target_vertices</code>	Optional world-space target vertices per tile (bottom face), used for target-based actuation.

**SimulationController: runtime state and stepping.** Two controllers drive the runtime behavior, each consuming the entries in `simulation_data`:

- Stepping: When `step_simulation()` is called, if the simulation is not paused, it first calls the `apply_forces()` function (which selects the appropriate actuation model) and then calls `p.stepSimulation()`.
- State Management: It handles `reset_simulation()` by calling the function `initialize_simulation()` to rebuild the world from scratch.

**InteractionController: user input and visual feedback.** The InteractionController handles real-time user input from the mouse and provides visual feedback. It also uses `simulation_data` to identify which objects are part of the kirigami structure.

- Mouse Events: In `process_mouse_events()`, it performs a ray cast from the camera through the mouse cursor. If the ray hits an object whose ID is in the bricks list from `simulation_data`, it triggers the pin/unpin action.
- Data Output: An OBJ file is exported.

**Main loop.** The entry point `run_sim.py` wires everything together and runs an interactive loop. The core structure is given in Algorithm 3:

---

**Algorithm 3** Interactive main loop

---

```

1: Initialize physics, Simulation, SimulationController, InteractionController
2: while Bullet client is connected do
3:   keys ← getKeyboardEvents()
4:   for each (key, handler) in handlers do
5:     if key was triggered then
6:       call handler()
7:       if key == 'q' then
8:         break loop
9:       end if
10:    end if
11:  end for
12:  InteractionController.process_mouse_events()
13:  SimulationController.step_simulation()
14:  sleep(timestep)
15: end while
16: disconnect()

```

---

For completeness and reproducibility, we summarize the default interactive controls used in PyKirigami’s GUI mode. These inputs allow manual actuation, dynamic boundary condition changes, camera manipulation, and on-demand export. Key bindings can be customized in the codebase; the mappings shown in Table 2 reflect the default configuration used in this paper.

Table 2: **Interactive Control Scheme for the PyKirigami Simulator.**

Control Input	Functionality
Left-click + drag	Apply external, damped forces to tiles for manual guidance and actuation during deployment.
Right-click	Toggle fixed-world constraints on a selected tile.
Space bar	Toggle pause/resume the physics simulation.
R	Reset the simulation to its initial configuration.
O	Export the result as an OBJ file.
Q	Quit the simulation application.
Scroll / Ctrl+drag	Zoom, rotate, and pan the camera for detailed visual inspection.

## B.5 Physical Environment Construction: CLI Parameters and Defaults

This section documents the primary command-line interface (CLI) flags used to configure and run the simulations. The table below groups related parameters and lists their default values and usage. For simplicity and portability, input files can be organized into a single directory within the `data/` folder and loaded using the `--model` flag. The CLI parameters and default values are given in Table 3:

## C Example Configurations and Simulation Details

In the main text, we presented several 2D-to-2D, 2D-to-3D, and 3D-to-3D deployments obtained with PyKirigami. Here we provide additional snapshots and, crucially, the corresponding physical environment and solver settings used for each case so that readers can reproduce the results precisely. All CLI flags follow Table 3. All simulations were run with a fixed timestep  $\Delta t = 1/240$  s and  $n_{\text{sub}} = 20$  internal substeps unless otherwise noted.

### C.1 Example: 2D-to-2D Square-to-Circle Kirigami Model

The 2D-to-2D square-to-circle kirigami model example (Fig. 10; see also main text Fig. 3a) demonstrates a robust setup for a 2D radial expansion. The primary challenge is to enforce planar motion and prevent the structure from buckling out-of-plane. Our strategy combines hinge kinematics with specific environmental and geometric settings, driven by an automated radial force model.

**Key Simulation Parameters.** A stable, planar, and automated deployment is achieved with the following configuration:

- **Kinematic Model:** We use **hinge joints** to connect the tiles. This is the most important choice, as it constrains tile rotation to the Z-axis, fundamentally preventing

Table 3: **Command-Line Interface (CLI) parameters and default values.** Parameter groups are distinguished by alternating background colors.

Flag	Default	Description
<i>Model and File Configuration</i>		
--model	(none)	Specifies a model folder <code>data/&lt;name&gt;/</code> containing input files like <code>vertices.txt</code> , <code>constraints.txt</code> and optional <code>target.txt</code> .
<i>Simulation Control and Stepping</i>		
--timestep	1/240	Fixed timestep $\Delta t$ per outer simulation step (s).
--substeps	20	Internal solver substeps $n_{\text{sub}}$ per outer step.
<i>Physical Environment</i>		
--gravity	0	Gravitational acceleration in $-z$ ( $\text{m/s}^2$ ).
--ground_plane	(switch)	Adds a visible ground plane to the simulation.
--ground_friction	0.5	Ground lateral friction coefficient $\mu_{\text{ground}}$ .
--linear_damping	0.05	Body linear velocity damping factor (per substep).
--angular_damping	0.05	Body angular velocity damping factor (per substep).
<i>Actuation Model</i>		
--cm_expansion	(switch)	Enables center-of-mass radial expansion force model.
--spring_stiffness	500	Vertex spring stiffness $k_s$ for target-based forces.
--force_damping	50	Actuator (viscous) damping $\mu_v$ for target-based forces.
<i>Geometry and Visualization</i>		
--brick_thickness	0.02	Thickness of extruded tiles (m).
--camera_distance	8.0	Initial camera distance from origin.

out-of-plane tumbling.

- **Actuation Model:** The deployment is driven by the automated Center-of-Mass Expansion model (`--cm_expansion`). No target file is needed.
- **Physical Environment:** `--gravity -200`, `--ground_plane`
- **Geometry:** `--brick_thickness 0.5`. This provides the tiles with rotational inertia to resist torsional instabilities.

## C.2 Example: 2D-to-2D Square-to-Disk Kirigami Model (Interactive Workflow)

Fig. 11 demonstrates the fully interactive workflow for the 2D-to-2D compact reconfigurable square-to-disk model shown in main text Fig. 3b. While the main text analyzes this structure’s automated deployment, here we show how to achieve the same reconfiguration manually

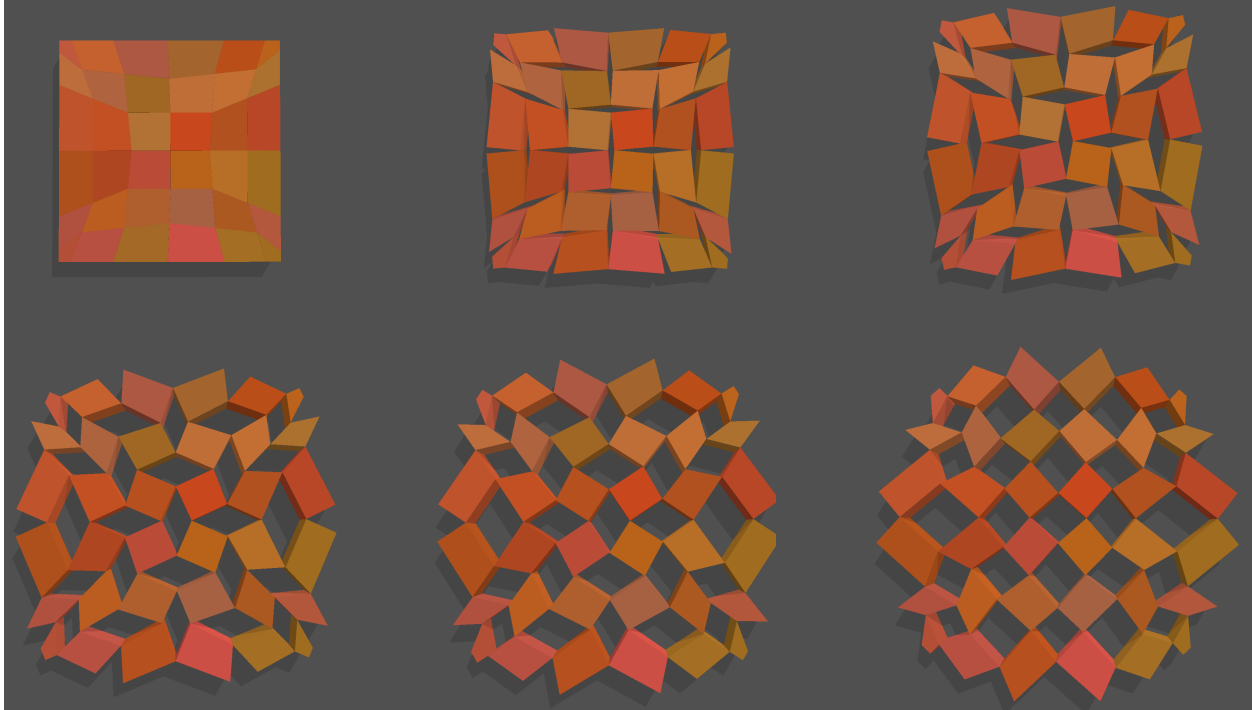


Figure 10: **Additional snapshots of the 2D-to-2D deployment of the square-to-circle kirigami model achieved by PyKirigami.**

using the GUI controls detailed in Table 2. This process highlights the use of the simulator for hands-on exploration and state capture.

With the simulation running in a no-force mode, a user can manually reconfigure the structure from the “square” to the “disk” state. This is achieved by applying the interactive controls from Table 2 in a strategic sequence, as illustrated in Fig. 11.

#### **Key Simulation Parameters:**

- **No Scripted Actuation:** To enable manual control, we launch the simulation without any automated force models. This is done by omitting the `--cm_expansion` flag and ensuring no `--target_vertices_file` is specified.
- **Physical Environment:** `--gravity -200 --ground_plane`
- **Visualization** `--brick_thickness 0.5`.

### **C.3 Example: 2D-to-3D Square-to-Spherical-Cap Kirigami Model**

The square-to-spherical-cap kirigami model example (Fig. 12; see also main text Fig. 3c) demonstrates a 2D-to-3D transformation from a flat sheet into a curved surface. This complex, out-of-plane motion is impossible to guide with simple radial forces and necessitates the use

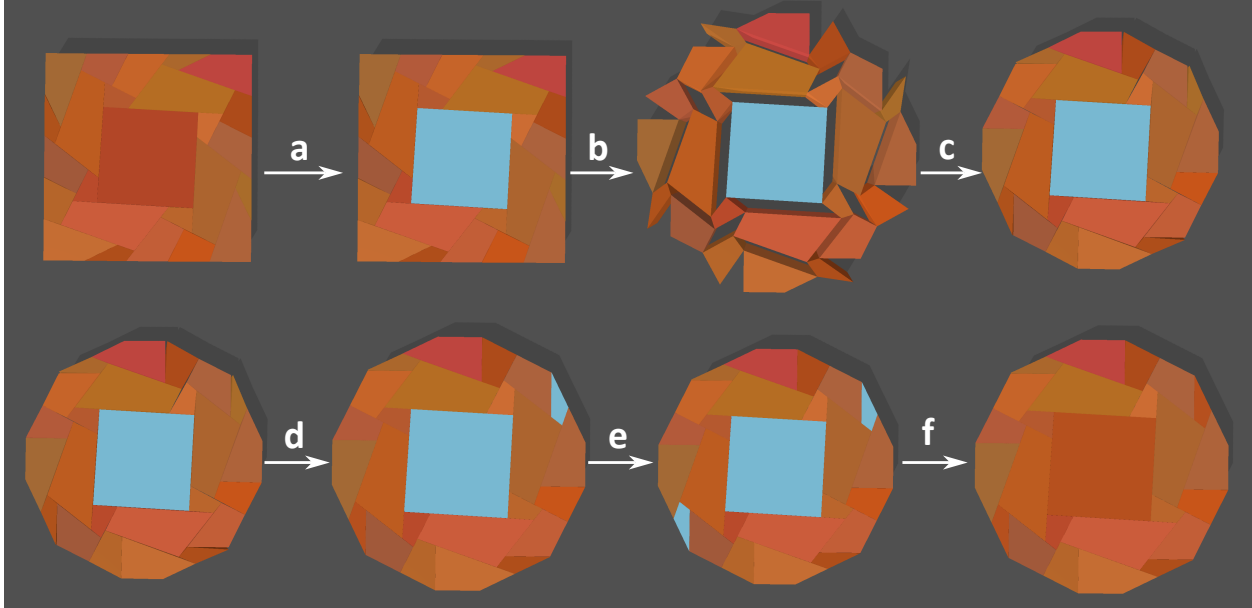


Figure 11: **Interactive workflow for the manual reconfiguration of the square-to-disk kirigami model.** **a**, A central tile is pinned (**Right-click**) to create a stable reference frame. **b**, An outer tile is dragged (**Left-click + drag**) to begin the radial expansion. **c**, The structure is guided into an approximate “disk” shape. At this stage, small gaps often persist due to the implicit hinge forces. **d**, To close a gap, a tile is dragged into the correct position through **Left-click + drag** and the simulation is then paused (**Space bar**), and the tile is pinned (**Right-click**) while paused. This “pause-and-pin” technique is a powerful feature, allowing a constraint to be applied to a desired geometry before the physics solver can react. **e**, Step **d** is repeated for other misaligned tiles. **f**, All pins are removed while paused, leaving the structure in a stable and precisely “disk” state.

of the target-based actuation model for precise control. Here, additional snapshots showing the progression from a planar to a spherical configuration are provided. Also, one can notice that out-of-plane motion provides extra degrees of freedom, allowing the sheet to lift/twist to resolve incompatibilities which can be seen in [20].

### Key Simulation Parameters:

- **Kinematic Model:** We use **spherical joints** to connect the bottom face of the tiles, allowing for the necessary three-dimensional rotational freedom.
- **Actuation Model:** The deployment is driven by the **Target-Based model**, with a target file defining the final spherical geometry.
- **Key Actuation Parameters:** `--spring_stiffness 400, --force_damping 50`.
- **Physical Environment:** `--ground_plane`. It can serve as a background to visualize the shadow.

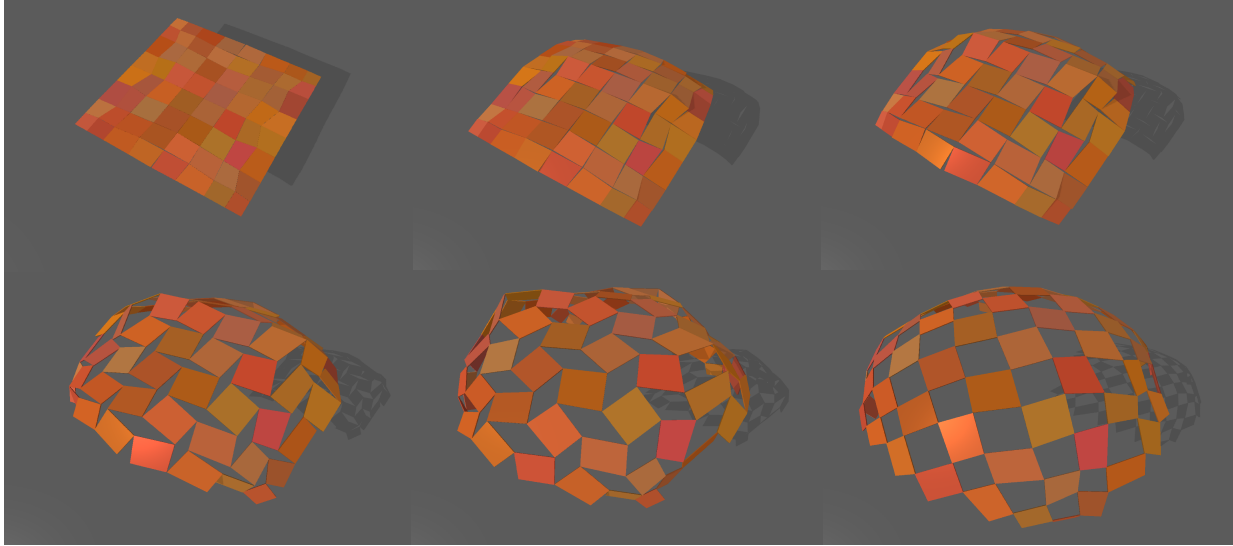


Figure 12: Additional snapshots of the 2D-to-3D deployment of the square-to-spherical-cap kirigami model achieved by PyKirigami, driven by the target-based force model.

- **Geometry:** `--brick_thickness 0.02`. It is noteworthy that if the tiles are too thick, they will block the deployment.

#### C.4 Example: 3D-to-3D Compact Reconfigurable Cylinder Kirigami Model

The 3D-to-3D compact reconfigurable cylinder kirigami model example (Fig. 13; see also main text Fig. 3d) involves the reconfiguration between two distinct 3D states, from a compact, folded cylinder to another compact, folded state. The target-based model is essential for guiding the structure through a collision-free volumetric transformation.

##### Key Simulation Parameters:

- **Kinematic Model:** We use **spherical joints** to allow for full 3D motion between the tiles.
- **Actuation Model:** The reconfiguration is driven by the **Target-Based model**.
- **Key Actuation Parameters:** `--spring_stiffness 300`, `--force_damping 50`.
- **Physical Environment:** `--gravity 0`
- **Geometry:** `--brick_thickness 0.02`. Note that thinner tiles yield a better deployment.

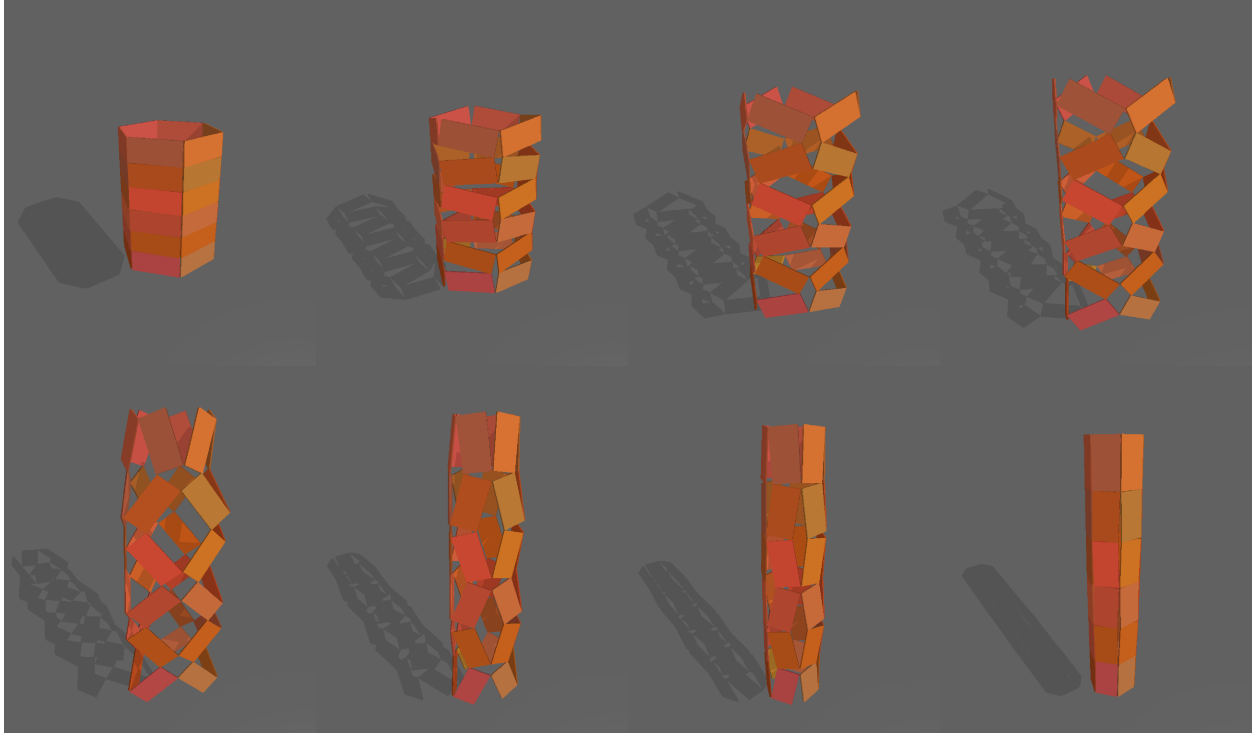


Figure 13: **Additional snapshots of the reconfiguration process of the 3D-to-3D cylinder kirigami structure achieved by PyKirigami.**

**A Note on Manual Exploration of 3D Structures.** Exploring the deployment of complex 3D structures manually can be challenging, as the structure may drift or collapse without a stabilizing force. A highly effective technique for stable manual exploration is to enable the target-based force model but set the **target vertices to be the initial vertices** of the structure, using a **very low spring stiffness** (e.g., `--spring_stiffness 50.0`). This setup creates a gentle “homing” force that pulls the structure back to its original configuration if left undisturbed, preventing it from drifting or collapsing. However, the spring force is weak enough that it can be easily overridden by the user with a manual drag (`Left-click + drag`). This allows the user to pull, twist, and probe the structure’s kinematic pathways safely. When the user releases the mouse, the structure will gently return to its stable initial state instead of collapsing chaotically. This “restoring spring” method provides a stable virtual testbed for hands-on analysis of complex 3D kirigami.

### C.5 Example: 2D-to-2D Stampfli Quasicrystal Kirigami Model

Note that the above kirigami structures primarily consist of quadrilateral tiles, and the overall structures exhibit a highly regular topology. To further demonstrate the applicability of PyKirigami to other kirigami structures, in Fig. 14 we show the deployment of a 12-fold Stampfli quasicrystal kirigami structure from [16]. Here, note that the structure contains not

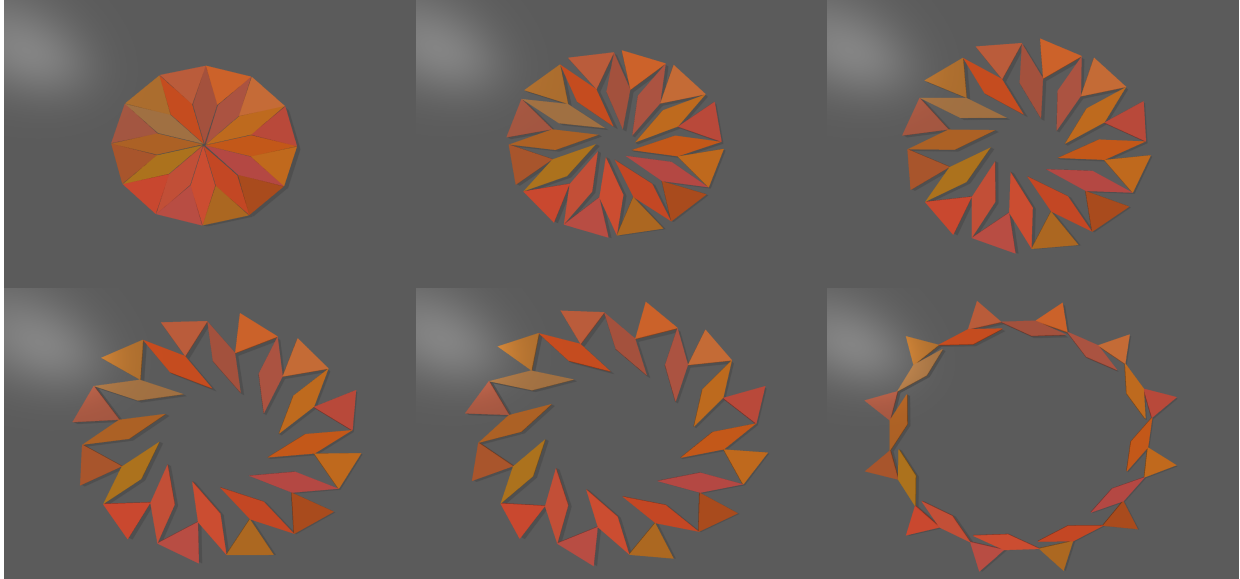


Figure 14: **The simulated deployment of the 12-fold Stampfli quasicrystal kirigami structure achieved by PyKirigami with automated radial expansion, stabilized by environmental forces.**

only quadrilateral tiles but also triangular tiles, and the tile connection is also highly different from the ones shown above. It can be observed that PyKirigami is capable of producing a deployment simulation of this structure with automated radial expansion.

**Key Simulation Parameters:** The physical environment and force model are the same as the ones in the previous 2D-to-2D square-to-circle example.

## C.6 Example: 2D-to-2D Compact Reconfigurable Fan Kirigami Model

To further demonstrate the versatility of PyKirigami, we present another example focusing on its interactive reconfiguration functionality. Fig. 15 shows the compact reconfigurable fan kirigami model, which has two different closed and compact contracted states. Users can apply the mentioned interactive operations to deploy it under the same physical environment as the square-to-disk model as shown in C.2.

## C.7 Example: 3D-to-3D cube-to-sphere Kirigami Model

Finally, we present a challenging 3D-to-3D transformation example using the cube-to-sphere kirigami model (Fig. 16; see also main text Fig. 1b). For this model, the six faces of the cube are deployed into a spherical approximation throughout the deployment process, which requires large, coordinated out-of-plane rotations and precise positioning to ensure the edges

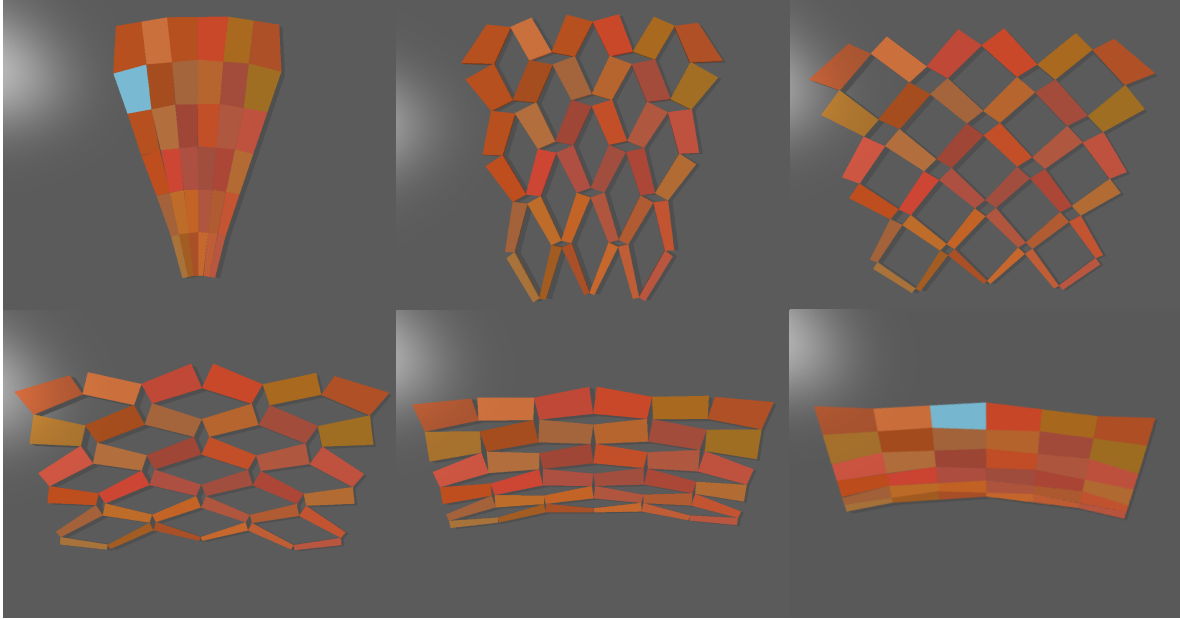


Figure 15: The simulated deployment of the compact reconfigurable fan kirigami model produced by PyKirigami with interactive shape morphing.

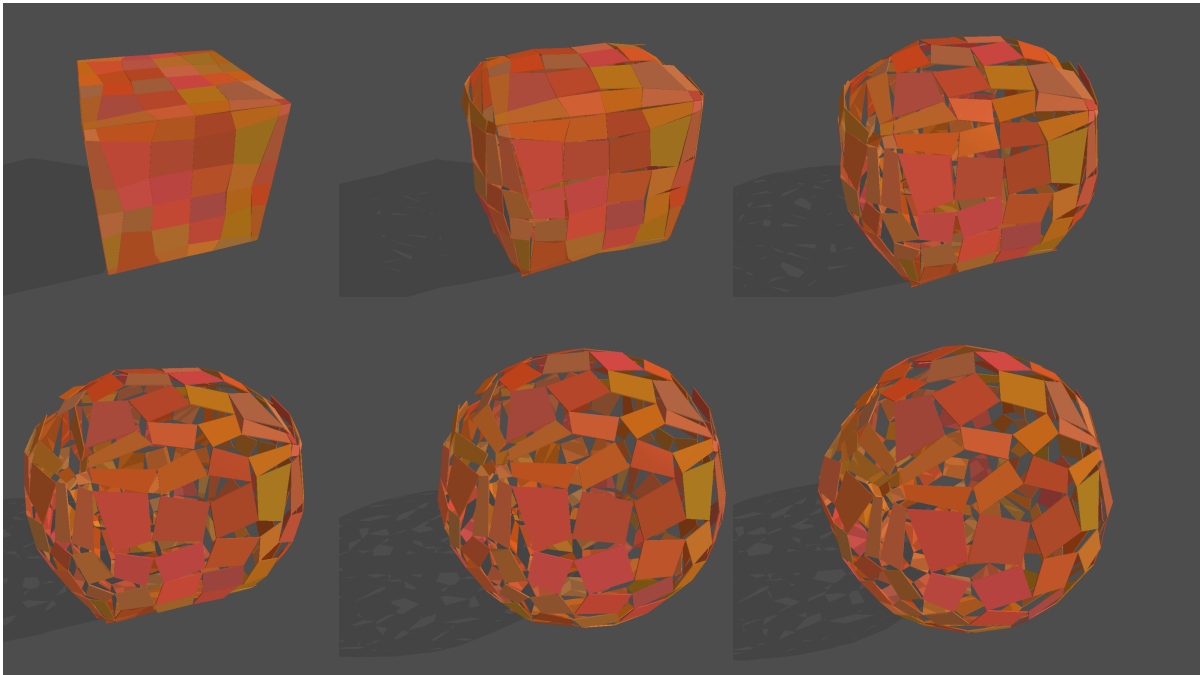


Figure 16: The simulated deployment of the cube-to-sphere kirigami model produced by PyKirigami. In this simulation, large, coordinated out-of-plane rotations and precise positioning are applied to control the deployment effect.

meet correctly without self-intersection. Such a transformation is infeasible with simple or manual forces and serves as a powerful demonstration of the target-based actuation model’s capabilities.

**Key Simulation Parameters:**

- **Actuation Model:** We use a modified **Target-Based model**. The core concept is to apply a stronger spring force to the central tiles of the face to drive the primary folding motion, while applying a weaker, gentler force to the outer, not totally constrained tiles. This hierarchical control strategy prevents the outer flaps from overshooting and significantly reduces final-state oscillations, ensuring a smooth and stable closure. This is a key advantage of PyKirigami’s flexible architecture, which allows users to easily implement custom force subclasses.
- **Visualization:** `--ground_plane`. To provide a better background of the 3D transformation, the ground is a little tilted by adjusting the view orientation during creation.

## D Analytic Kinematic Models for Quantitative Validation

To validate the numerical accuracy of PyKirigami, we derive the exact kinematic equations for the two benchmark kirigami structures used in main text. Both systems function as single-degree-of-freedom (1-DOF) mechanisms, where the global configuration is uniquely determined by the deployment angle  $\theta$ .

### D.1 Rectangular Tessellation

The rectangular tessellation is frequently used as a base case in kirigami design, and its analytical vertex position along with deployment angle  $\theta$  can be easily derived. As shown in Fig. 17a, the unit cell consisting of four rectangles has the size  $L \times W$  where

$$\begin{pmatrix} L \\ W \end{pmatrix} = 2 \begin{pmatrix} \sin(\eta) & \cos(\eta) \\ \cos(\eta) & \sin(\eta) \end{pmatrix} \begin{pmatrix} l \\ w \end{pmatrix}, \quad \eta = \theta/2,$$

assuming that the small rectangles have size  $l \times w$ .

### D.2 Square-to-Disk Kirigami Structure

The compact reconfigurable square-to-disk kirigami structure exhibits a more complex, non-linear kinematic path. The radial position  $R$  of boundary vertices is coupled to the deployment angle  $\theta$  (Fig. 17b). The position of all inner vertices  $\mathbf{v}_k$  in the assembly can be derived via a matrix multiplication

$$\mathbf{v}_k = MV,$$

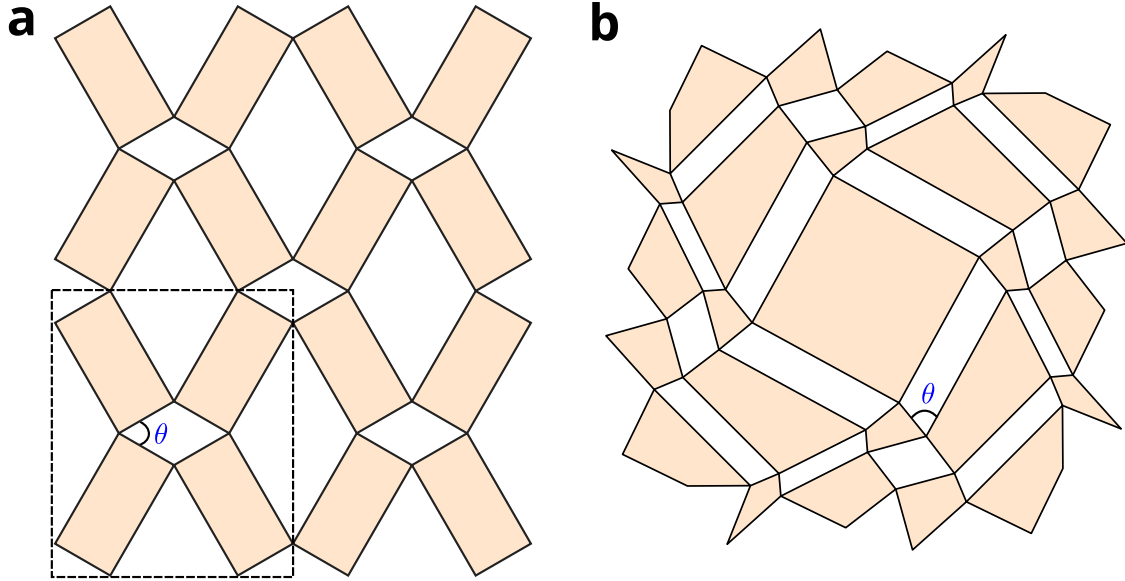


Figure 17: **The definition of the deployment angle in the benchmark cases.****a.** The rectangular tessellation kirigami structure. The dashed line shows a unit cell of the tessellation, in which the deployment angle  $\theta$  can be defined. **b.** The rigidly-deployable square-to-disk kirigami structure from [25], in which the deployment can be characterized by a single deployment angle  $\theta$ .

where the matrix  $M$  is related to the deployment angle and  $V$  are the seed vertices. More details can be found in [25].

## E Video Captions

**Supplementary Video 1:** The 2D-to-2D deployment of the square-to-disk kirigami model achieved by PyKirigami.

**Supplementary Video 2:** The 2D-to-3D deployment of the square-to-spherical-cap kirigami model achieved by PyKirigami.

**Supplementary Video 3:** The 3D-to-3D deployment and reconfiguration of the cylinder kirigami model achieved by PyKirigami.

**Supplementary Video 4:** The 3D-to-3D deployment of the cube-to-sphere kirigami model achieved by PyKirigami.